Earth-Science Reviews 177 (2018) 637–642

Contents lists available at ScienceDirect

Earth-Science Reviews

journal homepage: www.elsevier.com/locate/earscirev

Invited review

Incorporating the effects of photorespiration into terrestrial paleoclimate reconstruction

Brian A. Schubert[a,*], A. Hope Jahren[b]

[a] University of Louisiana at Lafayette, School of Geosciences, Lafayette, LA 70504, United States
[b] Centre for Earth Evolution and Dynamics, University of Oslo, N-0315 Oslo, Norway

A B S T R A C T

Paleoclimate reconstruction from the carbon stable isotopes in fossilized terrestrial organic matter relies upon a simple relationship between isotope discrimination and photosynthetic rate or leaf stomatal conductance (c_i/c_a). The carbon in plant tissues, however, represents the net carbon gained during photosynthesis, i.e., the balance of carbon gained through the stomata minus the carbon lost via photorespiration and respiration. While carbon isotope discrimination during respiration is negligible, ^{13}C discrimination during photorespiration can change plant isotope composition by several per mil. Our analysis of 123 *Arabidopsis thaliana* plants grown under a large range of subambient-to-highly-elevated pCO_2 revealed a positive response between carbon isotope discrimination and pCO_2 that was both consistent with the theoretical estimate for photorespiration and mathematically independent of c_i/c_a. Studies that seek to reconstruct climate records from plant-derived substrates must account for changes in atmospheric pCO_2 when attributing isotopic shifts to changes in photosynthetic rate or stomatal conductance driven by environmental conditions.

1. Introduction

The carbon stable isotope composition of fossilized terrestrial organic matter (δ_{TOM}) has become a widely measured (e.g., Nordt et al., 2016) proxy for ancient climate change (e.g., Kohn, 2010). Measured δ_{TOM} values are often used to reconstruct environmental conditions via the following equation description of isotope discrimination during photosynthesis, simplified from Farquhar et al. (1982b):

$$\Delta = a + (b–a)(c_i/c_a) \quad (1)$$

where Δ represents the isotopic difference between atmospheric CO_2 (δ_a) and plant tissue ($\delta_p \approx \delta_{TOM}$) [i.e., $\Delta = (\delta_a - \delta_p) / (1 + \delta_p)$], a represents the isotopic discrimination due to diffusion (a = 4.4‰), b is the isotopic discrimination by the enzyme RuBisCO (b = 26–30‰), and c_i/c_a represents a measure of photosynthetic rate or stomatal conductance, i.e., the ratio of intercellular CO_2 (c_i) to atmospheric CO_2 (c_a; $\approx pCO_2$).

Because a and b are constants, Eq. (1) suggests that any change in Δ must be attributed to a change in c_i/c_a. The primary mechanism by which plants change c_i/c_a value is by modulating the openness of the stomata, thus increasing or decreasing c_i relative to c_a. Because water evaporates through leaf stomata, plants maintain water balance by adjusting the stomatal conductance of their leaves, i.e., by changing c_i/c_a (e.g., Brodribb, 1996). Apparent correlations between δ_p and mean annual precipitation (MAP) have led some authors to argue that any change in δ_{TOM} is best interpreted as a change in paleo-environmental water-availability (Diefendorf et al., 2010; Kohn, 2010).

However, plant tissues are not simply constructed from assimilated CO_2. Instead, they are synthesized from the pool of net carbon captured during metabolism, i.e., the balance of carbon gain via assimilation and carbon loss via photorespiration and respiration. Because of this distinction, we contend here that values of δ_{TOM} are best interpreted using the complete equation of Farquhar et al. (1982b), which describes isotope discrimination during net carbon capture:

$$\Delta = a + (b–a)(c_i/c_a) – f(\Gamma^*)/c_a – e(R_d)/(k^*c_a) \quad (2)$$

where f represents discrimination during photorespiration, Γ^* is the CO_2 compensation point in the absence of dark respiration, e represents discrimination during respiration, R_d is the rate of dark respiration, and k is measure of the carboxylation efficiency. Thus, photorespiration and respiration are represented by the expressions $f(\Gamma^*)/c_a$ and $e(R_d)/(k^*c_a)$, respectively.

For this study, our goal was to quantify Δ across the full range of atmospheric pCO_2 that occurred during the entire history of land plant evolution, and interpret the results using the full description of net carbon capture (Eq. (2)). Our previous work quantified the relationship

* Corresponding author.
E-mail address: schubert@louisiana.edu (B.A. Schubert).

https://doi.org/10.1016/j.earscirev.2017.12.008
Received 16 May 2017; Received in revised form 17 November 2017; Accepted 14 December 2017
Available online 21 December 2017
0012-8252/

between Δ and pCO_2 across a wide range of elevated pCO_2 (Schubert and Jahren, 2012); however, for large intervals of the Phanerozoic [e.g., Neogene through today and Permo-Carboniferous glaciation] pCO_2 was lower than today (< 400 ppmv) (Foster et al., 2017; Royer, 2006), where ^{13}C discrimination is predicted to be most sensitive to changing pCO_2 (Schubert and Jahren, 2012). Here we extend these previous results by modifying our experimental growth chambers in order to maintain subambient pCO_2, while otherwise conferring the same temperature, light, and nutrient conditions as used in our previous experiments.

2. Methods

We grew a total of 60 *Arabidopsis thaliana* plants from seed to maturity under 5 different levels of subambient pCO_2 (97, 168, 246, 322 and 392 ppmv), with pO_2 maintained at ambient conditions (≈ 21%), and analyzed the above-ground tissues for δ_p value. These data, combined with that of the 63 other *A. thaliana* plants that we had grown within the same chambers under 7 different levels spanning elevated pCO_2 (370, 455, 733, 995, 1302, 1843, and 2255 ppmv) (Schubert and Jahren, 2012), represent a comprehensive dataset of δ_p values from plants grown across the full range of atmospheric pCO_2 hypothesized for the last 400 Myr (Royer, 2014) (Table S1).

The new experiments used the same flow-through growth chambers (122 cm × 91 cm × 46 cm), previously used to maintain elevated levels of pCO_2 relative to ambient (Hagopian et al., 2015; Schubert and Jahren, 2011; Schubert and Jahren, 2012). In order to achieve subambient levels of pCO_2 (< 392 ppmv) in these new experiments, we first removed all of the CO_2 from a compressed air supply by bleeding it through a scrubbing canister filled with 1000 g of 812 mesh Sofnolime (grade 797) carbon dioxide absorbent granules (Molecular Products, Ltd., Thaxted, Essex, UK). The resulting CO_2-free air-stream flowed into each growth chamber, creating a positive pressure and encouraging the flow-through system. At the airflow intake of each chamber, a very small amount of pure, beverage-grade CO_2 was added to CO_2-free air-stream until the pCO_2 value stabilized at the desired level, as confirmed by LI-840A CO_2 analyzers (LI-COR Biosciences, Lincoln, NE, USA) (Fig. 1a).

Each day of the experiment, the absorbent within the scrubbing canister was replaced two hours prior to the activation of the growth lights (i.e., two hours before "dawn"). On days 10 through 21 of the 22-day experiment, samples of air were collected in triplicate from within each chamber and analyzed for the $\delta^{13}C$ value of CO_2 (δ_a) using the direct injection method described within Hagopian et al. (2015). Average daily δ_a values are shown in Fig. 1b; the standard deviation of the three replicates never varied by > 0.05‰. The standard deviation of the δ_a value within each chamber over the course of the 12 sample days did not exceed ± 0.11‰ for any chamber (Table S1), and thus reflected the δ_a value within each chamber throughout the course of the plant growth experiments.

Within each chamber, twelve *A. thaliana* plants (Columbia, Col-0; Arabidopsis Biological Resource Center, The Ohio State University) were cultivated from seed to maturity (3 days to germination, followed by 22 days of growth). The plants were harvested prior to the initiation of flowering, in keeping with our previous protocol (Schubert and Jahren, 2012). Each plant occupied a separate 3 in × 3 in × 4 in (7.62 cm × 7.62 cm × 10.16 cm) container with standard potting soil (Miracle-Gro Moisture Control); no additional fertilizer was applied.

Water availability was kept constant throughout the experiment at a targeted gravimetric soil water content (θ_m; gram water per gram dry soil) = 1.87 g g^{-1} (65.2% water). This value of θ_m was then carefully maintained throughout the experiment: monitoring measurements (n = 2157 measurements) showed an average of 1.83 ± 0.05 g g^{-1} (64.6 ± 0.6% water) (Table S1); at no point during the experiment did any plant experience θ_m < 1.69 g g^{-1} (62.8% water) or θ_m > 1.89 g g^{-1} (65.4% water). Above ground, constant levels of relative humidity were maintained using a custom-built controlled feedback humidifier, and ranged from 64.0 ± 3.4 to 66.1 ± 2.4% (Table S1) (Fig. 1c).

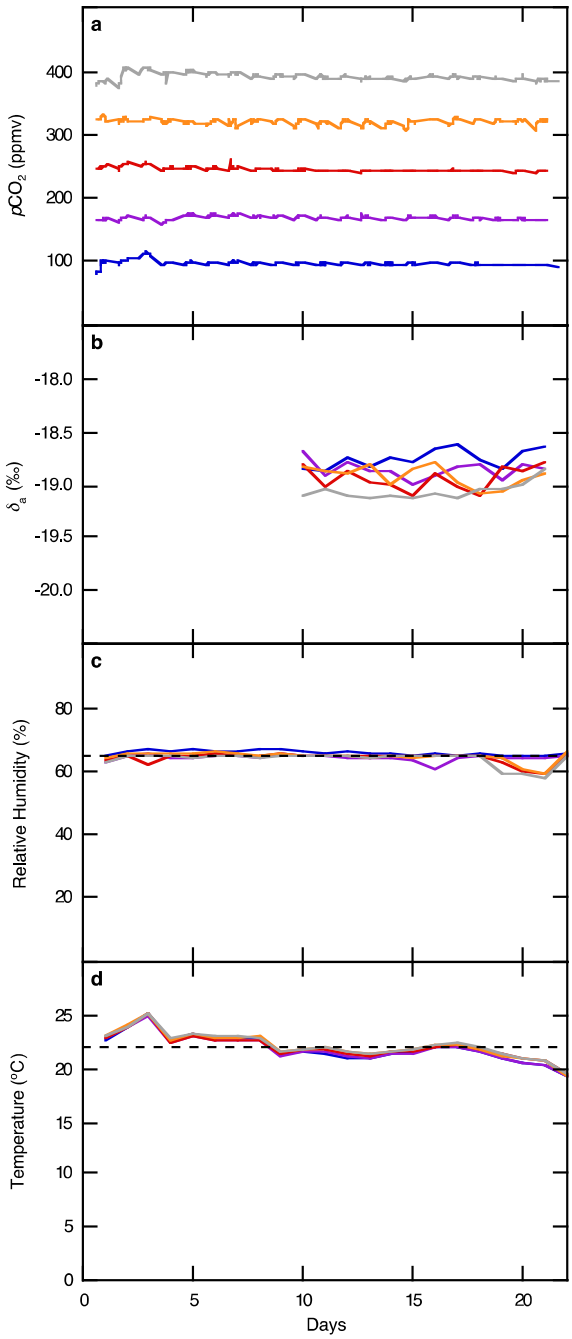

Fig. 1. pCO_2 (a), δ_a (b), relative humidity (c), and temperature (d) measured within each of the five, controlled growth chambers across the 22-day experiment. Black, dashed lines mark the average relative humidity and temperature conditions.

Light (i.e., photosynthetic photon flux) was maintained at 280 μmol m^{-2} s^{-1} (400–700 nm) for 12 continuous hours each day using fluorescent lamps (Phillips product #F32T8/TL841/ALTO). Plants were rotated daily within each chamber. Air temperature showed the expected diurnal cycle, but was highly consistent among chambers (Fig. 1d); average air temperature across the 22 days of growth (day and night) ranged from 21.9 ± 2.2 to 22.2 ± 2.2 °C, day temperature

ranged from 23.6 ± 1.2 to 24.0 ± 1.3 °C, and night temperature ranged from 20.2 ± 1.6 to 20.5 ± 1.4 °C (Table S1).

After 22 days of growth, above-ground tissues from each plant were harvested and dried at 60 °C, then homogenized using a mortar and pestle in preparation for stable isotope analysis. The $\delta^{13}C$ value of the above-ground tissues from each plant (δ_p) was analyzed using a Delta V Advantage Isotope Ratio Mass Spectrometer (Thermo Fisher, Bremen, Germany) coupled to a Costech ECS 4010 Elemental Analyzer with a zero-blank autosampler (Costech Analytical, Valencia, CA, USA). Each sample was analyzed in triplicate; the average standard deviation of the three replicates was 0.12‰ (median = 0.04‰); δ_p data, expressed in the δ-notation in units of per mil (‰), are presented in Table S1.

3. Results and discussion

In order to assess our experimental dataset, we sought to compare our measured values of Δ with the idealized values of Δ implied for our growth conditions by Eq. (2). While multiple studies have documented significant carbon isotope fractionation during photorespiration (e.g., Evans and von Caemmerer, 2013; Igamberdiev et al., 2004; Lanigan et al., 2008), the effect of respiration on Δ has been confirmed to be negligible within multiple works (e.g., Ghashghaie et al., 2003; Lin and Ehleringer, 1997; Lloyd and Farquhar, 1994), thus we initiated our analysis by modifying Eq. (2) to exclude the term describing respiration:

$$\Delta = a + (b-a)(c_i/c_a) - f(\Gamma^*)/c_a \quad (3)$$

This equation, which is consistent with Eq. (5) within Ubierna and Farquhar (2014), can be used when information on mesophyll conductance is lacking (it assumes that any rapid fluctuations in mesophyll conductance are averaged out on longer timescales), and, because mesophyll conductance can be difficult to estimate, represents a simplification of the comprehensive model (via assumption of infinite mesophyll conductance, i.e., the mesophyll contribution = 0) (ibid.).

We next performed an iterative optimization of all the variables simultaneously using Excel Solver (Frontline Systems Inc., Nevada, USA) to minimize the root mean squared error (RMSE) between the values of Δ that we obtained from our experiments and the idealized values of Δ arising from Eq. (3). We set all variables to be consistent with the literature, in order to specifically examine the value of discrimination during photorespiration (f) that the minimization implied. We allowed for the full range of possible c_i/c_a (= 0 to 1), and allowed b to range from 26 to 30‰ to span all previous estimates (Christeller et al., 1976; Farquhar et al., 1982a; Guy et al., 1993; Lloyd and Farquhar, 1994; Roeske and O'Leary, 1984; Suits et al., 2005; Wong et al., 1979). We fixed the CO_2 compensation point (Γ*) at 40 ppmv after multiple studies (Bernacchi et al., 2002; Bernacchi et al., 2001; Brooks and Farquhar, 1985; Kebeish et al., 2007; von Caemmerer, 2000; von Caemmerer et al., 1994). Experiments have indicated that elevated pCO_2 may increase leaf temperature (e.g., average increase = 0.2 °C: 375 to 550 ppmv) (Bernacchi et al., 2007; O'Neill et al., 2011), but such changes (i.e., 1.4 °C per 10^3 ppmv) have an insignificant effect on Γ* (Bernacchi et al., 2002).

The lowest value of RMSE (i.e., the "best fit") resulted when f = 9.1‰ (Fig. 2); this value falls within the range of reported values from current estimates for discrimination during photorespiration (Table 1). This curve resulted when c_i/c_a remained a constant [$c_i/c_a = (45.47)(b)^{-1.187}$] (Fig. 3), consistent with the recent work of Keeling et al. (2017). Thus no change in c_i/c_a was required to drive a ~3.5‰ increase in Δ across ~100 to 2250 ppmv. This yields the important result that pCO_2 can affect carbon isotope discrimination *independent* of c_i/c_a. To illustrate, Fig. 4a shows the relationship between Δ and pCO_2 under our best-fit estimate of f = 9.1‰ (with Γ* = 40 ppmv and b = 29.9‰). Note that higher or lower values for c_i/c_a can shift the curve in terms of the maximum value of Δ, but such a shift does not modify the fundamental response that we have measured.

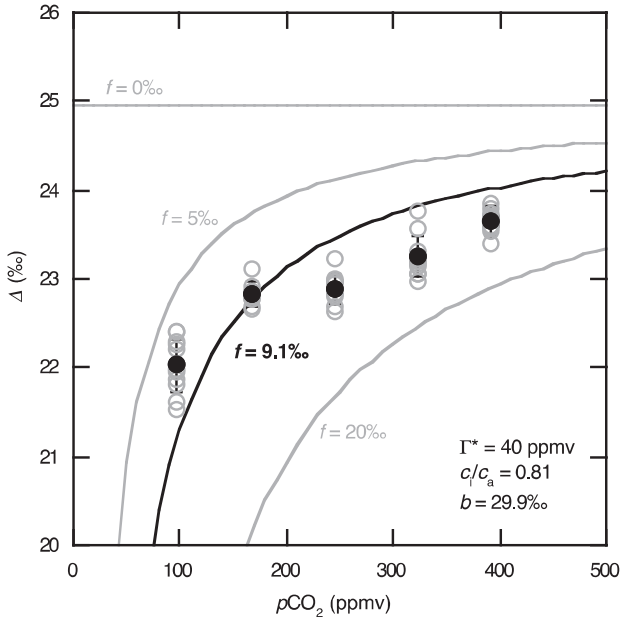

Fig. 2. The effect of photorespiration on the relationship between pCO_2 and Δ (modeled using Eq. (3)) across pCO_2 = 97 to 392 ppmv. Δ values for individual plants are shown by open gray circles; average Δ values for each pCO_2 are plotted as filled black circles (with 1σ error bars). For all curves, Γ* = 40 ppmv, c_i/c_a = 0.81, and b = 29.9‰. The best-fit curve through both subambient (this study) and elevated (Schubert and Jahren, 2012) pCO_2 experiments is obtained when f = 9.1‰ (bold black curve); f = 0‰, 5‰, and 20‰ are shown in gray for comparison. Identical curves result for any value for b chosen, provided that $c_i/c_a = (45.47)(b)^{-1.187}$ (Fig. 3). These curves all approach Δ = 24.94‰ at infinite pCO_2; however, the curves can be shifted up or down through a change in c_i/c_a (assuming a and b are held constant) (Eq. (3)) (Fig. 4a).

Table 1
Fractionation factors for photorespiration (f).

f (‰)	Species	Reference
9.1	*Arabidopsis thaliana*	This study
19.2	–[a]	This study
9.8 to 13.3	*Hordeum vulgare*	Igamberdiev et al. (2004)
10.2	*Arabidopsis thaliana*	Igamberdiev et al. (2004)
11.8 to 13.7	*Solanum tuberosum*	Igamberdiev et al. (2004)
14.5 to 22.0	*Nicotiana tabacum*	Evans and von Caemmerer (2013)
11.6 ± 1.5	*Senecio* spp.	Lanigan et al. (2008)
~10	–[a]	Ghashghaie et al. (2003)
~11	–[b]	Tcherkez (2006)

[a] Multiple species.
[b] Theoretical value.

In order to compare our experiments on *A. thaliana* with dozens of other plant species (including both angiosperms and gymnosperms) that were grown under variable pCO_2, we calculated the relative change in Δ (i.e., S = ‰/ppmv of pCO_2) for a wide range of C_3 species reported in the literature (Fig. 4b). The data showed a trend of decreasing S with increasing pCO_2 consistent our previous work on elevated pCO_2 (Fig. 3 within Schubert and Jahren, 2012), and verified that the effect of pCO_2 on Δ is greatest under subambient pCO_2.

In addition, by taking the first derivative of Eq. (3), we see that c_i, and thus c_i/c_a, has no effect on the slope of the curves (S), again reinforcing our claim that the relationship between Δ and pCO_2 is independent of photosynthetic rate or stomatal conductance:

$$S = (f)(\Gamma^*)(c_a^{-2}) \quad (4)$$

Eq. (4) also predicts that S is inversely proportional to c_a^2; therefore S decreases with increasing pCO_2, regardless of the absolute Δ value of

Table 2
The amount of discrimination per ppmv increase in pCO_2 (S) measured in C_3 land plants (updated from Schubert and Jahren, 2012; Schubert and Jahren, 2013; Schubert and Jahren, 2015).

S (‰/ppmv)	pCO_2 range (ppmv)	Species	Reference
0.0223	97–168	*Arabidopsis thaliana*	This study
0.0088	168–246	*Arabidopsis thaliana*	This study
0.0046	246–322	*Arabidopsis thaliana*	This study
0.0029	322–392	*Arabidopsis thaliana*	This study
0.0022	370–455	*Arabidopsis thaliana*	This study
0.0011	455–733	*Arabidopsis thaliana*	This study
0.00050	733–995	*Arabidopsis thaliana*	This study
0.00028	995–1302	*Arabidopsis thaliana*	This study
0.00015	1302–1843	*Arabidopsis thaliana*	This study
0.000087	1843–2255	*Arabidopsis thaliana*	This study
0.0080	380–760	*Arabidopsis thaliana*	Lomax et al. (2012)
0.0038	760–1000	*Arabidopsis thaliana*	Lomax et al. (2012)
0.0021	1000–1500	*Arabidopsis thaliana*	Lomax et al. (2012)
0.00060	2000–3000	*Arabidopsis thaliana*	Lomax et al. (2012)
0.0011	1500–2000	*Arabidopsis thaliana*	Lomax et al. (2012)
0.0075	360–700	*Arabidopsis thaliana*	Igamberdiev et al. (2004)
0.00082	700–1400	*Arabidopsis thaliana*	Igamberdiev et al. (2004)
0.0067	360–700	*Hordeum vulgare*	Igamberdiev et al. (2004)
0.00017	700–1400	*Hordeum vulgare*	Igamberdiev et al. (2004)
0.0120	285–365	*Juniperus* spp.	Treydte et al. (2009)
0.0142	296–366	*Larix sibirica*	Knorre et al. (2010)
0.0062	380–607	*Linaria dalmatica*	Sharma and Williams (2009)
0.0166	296–390	*Litsea calicaris*	Reichgelt et al. (2016)
0.0175	380–482	*Pinus contortus*	Sharma and Williams (2009)
0.0270	198–243	*Pinus flexilis*	Van de Water et al. (1994)
0.0220	243–279	*Pinus flexilis*	Van de Water et al. (1994)
0.0213	324–369	*Pinus sylvestris*	Betson et al. (2007)
0.0207	303–361	*Pinus sylvestris*	Berninger et al. (2000)
0.0100	343–569	*Quercus ilex*	Saurer et al. (2003)
0.0073	350–700	*Quercus petrea*	Kürschner (1996)
0.0096	407–497	*Raphanus sativus*	Schubert and Jahren (2012)
0.0072	497–576	*Raphanus sativus*	Schubert and Jahren (2012)
0.0048	576–780	*Raphanus sativus*	Schubert and Jahren (2012)
0.0020	780–1494	*Raphanus sativus*	Schubert and Jahren (2012)
0.00096	1494–1766	*Raphanus sativus*	Schubert and Jahren (2012)
0.00054	1766–2723	*Raphanus sativus*	Schubert and Jahren (2012)
0.00029	2723–3429	*Raphanus sativus*	Schubert and Jahren (2012)
0.00019	3429–4200	*Raphanus sativus*	Schubert and Jahren (2012)
0.0160	280–380	*Sabina przewalskii*	Wang et al. (2011)
0.0145	285–354	*Swietenia macrophylla*	Hietz et al. (2005)
0.0245	281–389	Mixed (n = 129)	Wu et al. (2017)
0.0200	300–310	Mixed (n = 11)	Peñuelas and Estiarte (1997)
0.0200	277–351	Mixed (n = 4)	Feng and Epstein (1995)
0.0188	310–350	Mixed (n = 11)	Peñuelas and Estiarte (1997)
0.0081	313–366	Mixed (n = 32)	Wang and Feng (2012)
0.0037	350–700	Mixed (n = 17)	Beerling and Woodward (1995)

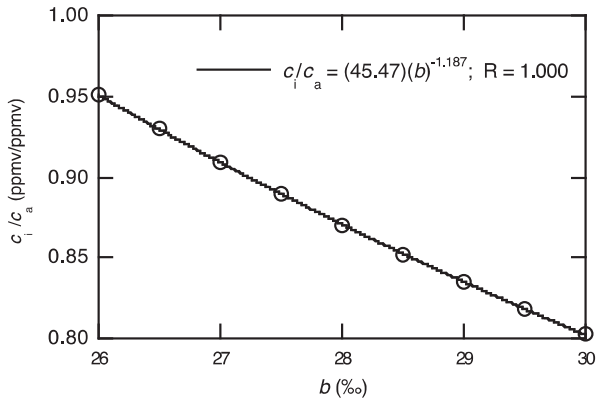

Fig. 3. The relationship between b and c_i/c_a determined by minimizing the root mean squared error (RMSE) between the values of Δ that we obtained from our experiments and the idealized values of Δ arising from Eq. (3) for b = 26 to 30‰ (at 0.5‰ increments). The same, lowest RMSE is determined for any b, provided that $c_i/c_a = (45.47)(b)^{-1.187}$.

the plant or the environment in which the plant was growing. This result is consistent with all available data; we note that the best fit for all species is obtained when f = 19.2‰ (Fig. 4b), which falls within the range of published estimates for discrimination during photorespiration (Table 1).

4. Conclusions

Our experiments growing the model plant *A. thaliana* under controlled and unchanging environmental conditions and across the full range of pCO_2 experienced by plants for the last 400 million years of Earth history (e.g., Franks et al., 2014) revealed an increase in Δ of ~3.5‰ that we attribute to the concomitant increase of pCO_2. The magnitude of the observed fractionation is consistent with that measured and modeled for photorespiration, the process by which previously fixed glycine is carboxylated to CO_2 within the mitochondrion. Photorespiration serves to decrease the overall efficiency of photosynthesis, and thus reduces the net amount of carbon available for the construction of plant tissues; rates of photorespiration have long been known to decrease with increasing pCO_2 (Sharkey, 1988).

The process of photorespiration is fundamental to all photosynthetic

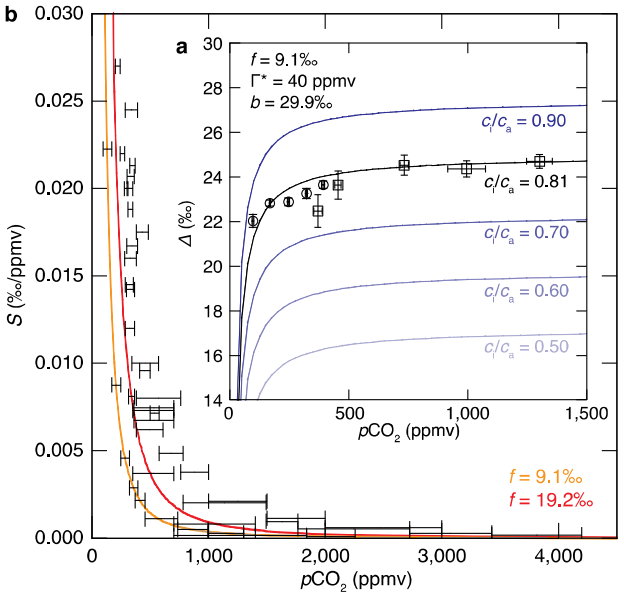

Fig. 4. The relationship between carbon isotope discrimination and atmospheric pCO_2. (a) The isotopic discrimination between atmospheric CO_2 (δ_a) and plant tissue (δ_p) [$\Delta = (\delta_a - \delta_p) / (1 + \delta_p)$] measured in *Arabidopsis thaliana* plants grown under subambient (○) and elevated (□) levels of pCO_2. For all curves, the value for *a*, *b*, *f*, and Γ* remain the same, while the value of c_i/c_a was allowed to range from 0 to 1 (Eq. (3)). The best-fit curve occurs with $c_i/c_a = 0.81$, consistent with the non-stressed conditions of the plants growing within the chambers (e.g., Fig. 2 within Cernusak et al., 2013). Note that regardless of the value for c_i/c_a, Δ is predicted to increase with increasing pCO_2, but Δ values > ~25‰ are likely rare, and require plants growing under ideal conditions and minimal rates of photorespiration (high pCO_2). When combining the results from our elevated and subambient experiments, it becomes apparent that the Δ value determined at $pCO_2 = 370$ ppmv is anomalously low; however, exclusion of this data point has minimal effect on the best-fit curve (*f* increases by only 0.1‰). (b) The effect of pCO_2 on Δ, reported as the change in Δ per change in pCO_2 (*S*, ‰/ppmv) (Eq. (4)). Horizontal bars encompass the range of pCO_2 variation within each experiment. Two curves are shown: $f = 9.1$‰ (orange; based on *A. thaliana*) and $f = 19.2$‰ (red; best-fit curve through multiple angiosperm and gymnosperm species, Table 2).

organisms; it occurs downstream from stomatal diffusion, after previously fixed carbon is transformed into glycine within the peroxisome. Photorespiration cannot be mediated through changes in photosynthetic rate or stomatal conductance, nor can it be mitigated through acclimation to changing pCO_2; it has persisted across all evolutionary timescales that include C_3 photosynthesis. Decreased isotopic discrimination due to photorespiration can be large, especially at low levels of pCO_2, or alternatively, at low ratios of atmospheric CO_2:O_2; however, recent experimental work has shown that Δ is primarily influenced by changes in pCO_2 as opposed to pO_2 (Porter et al., 2017). For these reasons, we contend that the interpretation of δ_{TOM} records must account for the dependence of Δ upon pCO_2, which is separate from the effect of climatic changes on photosynthetic rate or stomatal conductance (c_i/c_a) (Eq. (3)). Considering the effect of photorespiration upon δ_{TOM} value is particularly important across the many intervals of the geologic record with known changes in atmospheric pCO_2 level, including current studies that seek to interrogate the effects of rising pCO_2 during the Anthropocene.

Acknowledgments

We thank W.M. Hagopian and Robert A. Graper for laboratory assistance. This material is based upon work supported by the U.S. Department of Energy under awards DE-FG02-13ER16412 (B.A.S.) and DE-FG02-09ER16002 (A.H.J.), and the Research Council of Norway through its Centers of Excellence funding scheme, Project # 223272 (A.H.J.).

References

Beerling, D.J., Woodward, F.I., 1995. Leaf stable carbon isotope composition records increased water-use efficiency of C_3 plants in response to atmospheric CO_2 enrichment. Funct. Ecol. 9 (3), 394–401.

Bernacchi, C.J., Kimball, B.A., Quarles, D.R., Long, S.P., Ort, D.R., 2007. Decreases in stomatal conductance of soybean under ppen-air elevation of [CO_2] are closely coupled with decreases in ecosystem evapotranspiration. Plant Physiol. 143 (1), 134–144.

Bernacchi, C.J., Portis, A.R., Nakano, H., von Caemmerer, S., Long, S.P., 2002. Temperature response of mesophyll conductance. Implications for the determination of Rubisco enzyme kinetics and for limitations to photosynthesis *in vivo*. Plant Physiol. 130 (4), 1992–1998.

Bernacchi, C.J., Singsaas, E.L., Pimentel, C., Portis Jr., A.R., Long, S.P., 2001. Improved temperature response functions for models of Rubisco-limited photosynthesis. Plant Cell Environ. 24 (2), 253–259.

Berninger, F., Sonninen, E., Aalto, T., Lloyd, J., 2000. Modeling ^{13}C discrimination in tree rings. Glob. Biogeochem. Cycles 14 (1), 213–223.

Betson, N.R., Johannisson, C., Löfvenius, M.O., Grip, H., Granström, A., Högberg, P., 2007. Variation in the $\delta^{13}C$ of foliage of *Pinus sylvestris* L. in relation to climate and additions of nitrogen: analysis of a 32-year chronology. Glob. Chang. Biol. 13 (11), 2317–2328.

Brodribb, T., 1996. Dynamics of changing intercellular CO_2 concentration (c_i) during drought and determination of minimum functional c_i. Plant Physiol. 111 (1), 179–185.

Brooks, A., Farquhar, G.D., 1985. Effect of temperature on the CO_2/O_2 specificity of ribulose-1,5-bisphosphate carboxylase/oxygenase and the rate of respiration in the light. Planta 165 (3), 397–406.

Cernusak, L.A., Ubierna, N., Winter, K., Holtum, J.A.M., Marshall, J.D., Farquhar, G.D., 2013. Environmental and physiological determinants of carbon isotope discrimination in terrestrial plants. New Phytol. 200 (4), 950–965.

Christeller, J.T., Laing, W.A., Troughton, J.H., 1976. Isotope discrimination by ribulose 1,5-diphosphate carboxylase: no effect of temperature or HCO_3^- concentration. Plant Physiol. 57, 580–582.

Diefendorf, A.F., Mueller, K.E., Wing, S.L., Koch, P.L., Freeman, K.H., 2010. Global patterns in leaf ^{13}C discrimination and implications for studies of past and future climate. Proc. Natl. Acad. Sci. U. S. A. 107 (13), 5738–5743.

Evans, J.R., von Caemmerer, S., 2013. Temperature response of carbon isotope discrimination and mesophyll conductance in tobacco. Plant Cell Environ. 36 (4), 745–756.

Farquhar, G.D., Ball, M.C., von Caemmerer, S., Roksandic, Z., 1982a. Effect of salinity and humidity on $\delta^{13}C$ value of halophytes: evidence for diffusional isotope fractionation determined by the ratio of intercellular/atmospheric partial pressure of CO_2 under different environmental conditions. Oecologia 52, 121–124.

Farquhar, G.D., O'Leary, M.H., Berry, J.A., 1982b. On the relationship between carbon isotope discrimination and the intercellular carbon dioxide concentration in leaves. Aust. J. Plant Physiol. 9, 121–137.

Feng, X., Epstein, S., 1995. Carbon isotopes of trees from arid environments and implications for reconstructing atmospheric CO_2 concentrations. Geochim. Cosmochim. Acta 59 (12), 2599–2608.

Foster, G.L., Royer, D.L., Lunt, D.J., 2017. Future climate forcing potentially without precedent in the last 420 million years. Nat. Commun. 8, 14845.

Franks, P.J., Royer, D.L., Beerling, D.J., Van de Water, P.K., Cantrill, D.J., Barbour, M.M., Berry, J.A., 2014. New constraints on atmospheric CO_2 concentration for the Phanerozoic. Geophys. Res. Lett. 41. http://dx.doi.org/10.1002/2014GL060457.

Ghashghaie, J., Badeck, F.-W., Lanigan, G., Nogués, S., Tcherkez, G., Deléens, E., Cornic, G., Griffiths, H., 2003. Carbon isotope fractionation during dark respiration and photorespiration in C_3 plants. Phytochem. Rev. 2 (1–2), 145–161.

Guy, R.D., Fogel, M.L., Berry, J.A., 1993. Photosynthetic fractionation of the stable isotopes of oxygen and carbon. Plant Physiol. 101 (1), 37–47.

Hagopian, W.M., Schubert, B.A., Jahren, A.H., 2015. Large-scale plant growth chamber design for elevated pCO_2 and $\delta^{13}C$ studies. Rapid Commun. Mass Spectrom. 29, 440–446.

Hietz, P., Wanek, W., Dünisch, O., 2005. Long-term trends in cellulose $\delta^{13}C$ and water-use efficiency of tropical *Cedrela* and *Swietenia* from Brazil. Tree Physiol. 25 (6), 745–752.

Igamberdiev, A.U., Mikkelsen, T.N., Ambus, P., Bauwe, H., Lea, P.J., Gardeström, P., 2004. Photorespiration contributes to stomatal regulation and carbon isotope fractionation: a study with barley, potato and *Arabidopsis* plants deficient in glycine decarboxylase. Photosynth. Res. 81, 139–152.

Kebeish, R., Niessen, M., Thiruveedhi, K., Bari, R., Hirsch, H.-J., Rosenkranz, R., Stabler, N., Schonfeld, B., Kreuzaler, F., Peterhansel, C., 2007. Chloroplastic photorespiratory bypass increases photosynthesis and biomass production in *Arabidopsis thaliana*. Nat. Biotechnol. 25 (5), 593–599.

Keeling, R.F., Graven, H.D., Welp, L.R., Resplandy, L., Bi, J., Piper, S.C., Sun, Y., Bollenbacher, A., Meijer, H.A.J., 2017. Atmospheric evidence for a global secular increase in carbon isotopic discrimination of land photosynthesis. Proc. Natl. Acad. Sci. 114 (39), 10361–10366.

Knorre, A.A., Siegwolf, R.T.W., Saurer, M., Sidorova, O.V., Vaganov, E.A., Kirdyanov, A.V., 2010. Twentieth century trends in tree ring stable isotopes ($\delta^{13}C$ and $\delta^{18}O$) of *Larix sibirica* under dry conditions in the forest steppe in Siberia. J. Geophys. Res. Biogeosci. 115 (G03002). http://dx.doi.org/10.1029/2009jg000930.

Kohn, M.J., 2010. Carbon isotope compositions of terrestrial C3 plants as indicators of (paleo)ecology and (paleo)climate. Proc. Natl. Acad. Sci. U. S. A. 107 (46), 19691–19695.

Kürschner, W.M., 1996. Leaf Stomata as Biosensors of Palaeoatmospheric CO_2 Levels.

Utrecht University, pp. 153.
Lanigan, G.J., Betson, N., Griffiths, H., Seibt, U., 2008. Carbon isotope fractionation during photorespiration and carboxylation in *Senecio*. Plant Physiol. 148 (4), 2013–2020.
Lin, G., Ehleringer, J.R., 1997. Carbon isotopic fractionation does not occur during dark respiration in C_3 and C_4 plants. Plant Physiol. 114 (1), 391–394.
Lloyd, J., Farquhar, G.D., 1994. ^{13}C discrimination during CO_2 assimilation by the terrestrial biosphere. Oecologia 99, 201–215.
Lomax, B.H., Knight, C.A., Lake, J.A., 2012. An experimental evaluation of the use of C_3 $\delta^{13}C$ plant tissue as a proxy for the paleoatmospheric $\delta^{13}CO_2$ signature of air. Geochem. Geophys. Geosyst. 13, Q0AI03.
Nordt, L., Tubbs, J., Dworkin, S., 2016. Stable carbon isotope record of terrestrial organic materials for the last 450 Ma yr. Earth Sci. Rev. 159, 103–117.
O'Neill, B.F., Zangerl, A.R., DeLucia, E.H., Casteel, C., Zavala, J.A., Berenbaum, M.R., 2011. Leaf temperature of soybean grown under elevated CO_2 increases *Aphis glycines* (Hemiptera: Aphididae) population growth. Insect Science 18 (4), 419–425.
Peñuelas, J., Estiarte, M., 1997. Trends in plant carbon concentration and plant demand for N throughout this century. Oecologia 109 (1), 69–73.
Porter, A.S., Yiotis, C., Montañez, I.P., McElwain, J.C., 2017. Evolutionary differences in $\Delta^{13}C$ detected between spore and seed bearing plants following exposure to a range of atmospheric O_2:CO_2 ratios; implications for paleoatmosphere reconstruction. Geochim. Cosmochim. Acta 213, 517–533.
Reichgelt, T., D'Andrea, W.J., Fox, B.R.S., 2016. Abrupt plant physiological changes in southern New Zealand at the termination of the Mi-1 event reflect shifts in hydroclimate and pCO_2. Earth Planet. Sci. Lett. 455, 115–124.
Roeske, C.A., O'Leary, M.H., 1984. Carbon isotope effects on the enzyme-catalyzed carboxylation of ribulose bisphosphate. Biochemistry 23, 6275–6284.
Royer, D.L., 2006. CO_2-forced climate thresholds during the Phanerozoic. Geochim. Cosmochim. Acta 70 (23), 5665–5675.
Royer, D.L., 2014. Atmospheric CO_2 and O_2 during the Phanerozoic: tools, patterns, and impacts. In: Turekian, K.K. (Ed.), Treatise on Geochemistry, Second Edition. Elsevier, Oxford, pp. 251–267.
Saurer, M., Cherubini, P., Bonani, G., Siegwolf, R., 2003. Tracing carbon uptake from a natural CO_2 spring into tree rings: an isotope approach. Tree Physiol. 23 (14), 997–1004.
Schubert, B.A., Jahren, A.H., 2011. Fertilization trajectory of the root crop *Raphanus sativus* across atmospheric pCO_2 estimates of the next 300 years. Agric. Ecosyst. Environ. 140 (1–2), 174–181.
Schubert, B.A., Jahren, A.H., 2012. The effect of atmospheric CO_2 concentration on carbon isotope fractionation in C_3 land plants. Geochim. Cosmochim. Acta 96, 29–43.
Schubert, B.A., Jahren, A.H., 2013. Reconciliation of marine and terrestrial carbon isotope excursions based on changing atmospheric CO_2 levels. Nat. Commun. 4 (1653). http://dx.doi.org/10.1038/ncomms2659.
Schubert, B.A., Jahren, A.H., 2015. Global increase in plant carbon isotope fractionation following the Last Glacial Maximum caused by increase in atmospheric pCO_2. Geology 43 (5), 435–438.
Sharkey, T.D., 1988. Estimating the rate of photorespiration in leaves. Physiol. Plant. 73 (1), 147–152.
Sharma, S., Williams, D.G., 2009. Carbon and oxygen isotope analysis of leaf biomass reveals contrasting photosynthetic responses to elevated CO_2 near geologic vents in Yellowstone National Park. Biogeosciences 6 (1), 25–31.
Suits, N.S., Denning, A.S., Berry, J.A., Still, C.J., Kaduk, J., Miller, J.B., Baker, I.T., 2005. Simulation of carbon isotope discrimination of the terrestrial biosphere. Glob. Biogeochem. Cycles 19 (GB1017).
Tcherkez, G., 2006. How large is the carbon isotope fractionation of the photorespiratory enzyme glycine decarboxylase? Funct. Plant Biol. 33 (10), 911–920.
Treydte, K.S., Frank, D.C., Saurer, M., Helle, G., Schleser, G.H., Esper, J., 2009. Impact of climate and CO_2 on a millennium-long tree-ring carbon isotope record. Geochim. Cosmochim. Acta 73, 4635–4647.
Ubierna, N., Farquhar, G.D., 2014. Advances in measurements and models of photosynthetic carbon isotope discrimination in C_3 plants. Plant Cell Environ. 37 (7), 1494–1498.
Van de Water, P.K., Leavitt, S.W., Betancourt, J.L., 1994. Trends in stomatal density and $^{13}C/^{12}C$ ratios of *Pinus flexilis* needles during last glacial-interglacial cycle. Science 264, 239–243.
von Caemmerer, S., 2000. Biochemical Models of Leaf Photosynthesis. Techniques in Plant Sciences (No. 2). CSIRO Publishing, Collingwood, Australia.
von Caemmerer, S., Evans, J.R., Hudson, G.S., Andrews, T.J., 1994. The kinetics of ribulose-1,5-bisphosphate carboxylase/oxygenase in vivo inferred from measurements of photosynthesis in leaves of transgenic tobacco. Planta 195 (1), 88–97.
Wang, G., Feng, X., 2012. Response of plants' water use efficiency to increasing atmospheric CO_2 concentration. Environ. Sci. Technol. 46 (16), 8610–8620.
Wang, W., Liu, X., Shao, X., Leavitt, S., Xu, G., An, W., Qin, D., 2011. A 200 year temperature record from tree ring $\delta^{13}C$ at the Qaidam Basin of the Tibetan Plateau after identifying the optimum method to correct for changing atmospheric CO_2 and $\delta^{13}C$. J. Geophys. Res. 116, G04022.
Wong, W.W., Benedict, C.R., Kohel, R.J., 1979. Enzymic fractionation of the stable carbon isotopes of carbon dioxide by ribulose-1,5-bisphosphate carboxylase. Plant Physiol. 63, 852–856.
Wu, M.S., Feakins, S.J., Martin, R.E., Shenkin, A., Bentley, L.P., Blonder, B., Salinas, N., Asner, G.P., Malhi, Y., 2017. Altitude effect on leaf wax carbon isotopic composition in humid tropical forests. Geochim. Cosmochim. Acta 206, 1–17.